CHIN. PHYS. LETT. Vol. 32, No. 12 (2015) 124303

The $V(z)$ Inversion Technique for Evaluation of an Adhesively Bonded Structure *

LIU Jing(刘婧)[1,2,3], XU Wei-Jiang(徐卫疆)[1**], HU Wen-Xiang(胡文祥)[2],
OURAK Mohamed[1], DUBOIS Andre[3]

[1]*Institut d'Electronique de Microélectronique et de Nanotechnologie, UMR CNRS 8520, Département DOAE, Université de Valenciennes, Valenciennes 59313, France*
[2]*Institute of Acoustics, Tongji University, Shanghai 200092*
[3]*Laboratoire d'Automatique de Mécanique et d'Informatique Industrielles et Humaines, UMR CNRS 8201, Université de Valenciennes, Valenciennes 59313, France*

(Received 21 September 2015)

Based on the fact that the evolution trace in incident angle and frequency of the resonance zeros of the reflection coefficient function for a water charged layered medium is equivalent to its guided wave mode dispersion, the interfacial adhesion of a three-layer aluminum–adhesive–aluminum bonding structure is characterized nondestructively by determining the interface shear stiffness k_t associated with the interfacial strength. The resonance reflection function is obtained experimentally by the $V(z)$ inversion technique using an ultrasonic focused transducer of wide-band and large angular aperture (up to $\pm 45^\circ$). The dispersion curves are numerically calculated, adjusting the parameter k_t so that the difference between the dispersion curves and the angular-frequency tracing of the reflection zeros is minimum. The parameter k_t at an interface of weakly adhered aluminum epoxy-resin is estimated to be 10^{14} N/m^3.

PACS: 43.40.Le, 43.35.Cg, 43.58.−e DOI: 10.1088/0256-307X/32/12/124303

The prediction of adhesion force at solid interfaces has important significance for both the understanding of its physical mechanisms[1,2] and the utilization of bonding technique for material assembly that is widely used in fabrication industries.[3] However, despite the great efforts made, the evaluation of material adhesion, especially interface adhesion, in a nondestructive way has been a challenge for a long time. No technique has been really available for its quantitative measurement. Ultrasonic technique seems to be the only possible approach for its nondestructive evaluation due to the mechanical nature of both the ultrasound and the adhesion phenomenon.[4]

An adhesively bonded structure is often a three-layer sandwich. Its adhesion force depends on two factors: the cohesive strength and the interfacial bonding strength. Usually the interfacial failure occurs before the cohesive one and thus is primordial to the structure strength. However its evaluation by using the bulk wave reflection is much more difficult due to the high acoustical impedance contrast between adhesive and adherend. It has been shown that the shear wave can be much more sensitive than the compression wave to a weak interface,[5] while the use of a shear wave transducer will encounter the coupling problem. The technique to generate a shear wave by mode conversion at the interface by using a compression wave at oblique incidence needs very complicated experimental disposition.[6]

This work uses ultrasonic guided mode waves to characterize the interface stiffness parameter by measuring the resonance mode dispersion. Compared with the echography technique, the above-mentioned sensibility and measurement difficulties could be improved for the reasons that the resonance modes are the wave resonance in layer thickness, formed by the multirefection between the extremities (interfaces or surfaces) of a layer and depending on both the layer properties and the interface conditions. For certain modes, there is concentration of both compression and shear stresses along the interface.

We first establish the wave propagation model for a multilayered structure, describing the boundary conditions of a weak interface by two interfacial normal and shear stiffness parameters k_n and k_t.[7] The plane wave angular (incident angle) and frequency reflection coefficient function $R(\theta, f)$ for a liquid immersed multilayer and its dispersion curves of guided mode waves with or without charge can be calculated. If the density of the charging liquid is several times smaller than that of the structure, the minima presented in the reflectance function (in its modulus) are equivalent to the structure resonances. Their evolutions in the angular and frequency plane coincide with the dispersion curves of the guided waves.[8] Based on this assumption, we secondly use a focused wave technique, also called the $V(z)$ inversion technique, permitting the reconstruction of the reflection function $R(\theta, f)$. Comparing the measured $R(\theta, f)$ with the calculated dispersion curves, the interface adhesion can be evaluated by adjusting the interfacial stiffness parameters in a way that the differences between the dispersion

*Supported by the Key Program of the National Natural Science Foundation of China under Grant Nos 10834009 and 11374230
**Corresponding author. Email: weijiang.xu@univ-valenciennes.fr

curves and zero $R(\theta, f)$ are minimum. Some research has confirmed that the normal interfacial stiffness $k_{\rm n}$ is less sensitive to the interface adhesion, especially to a slip interface, so only the shear stiffness $k_{\rm t}$ has been taken into consideration in this study.[9]

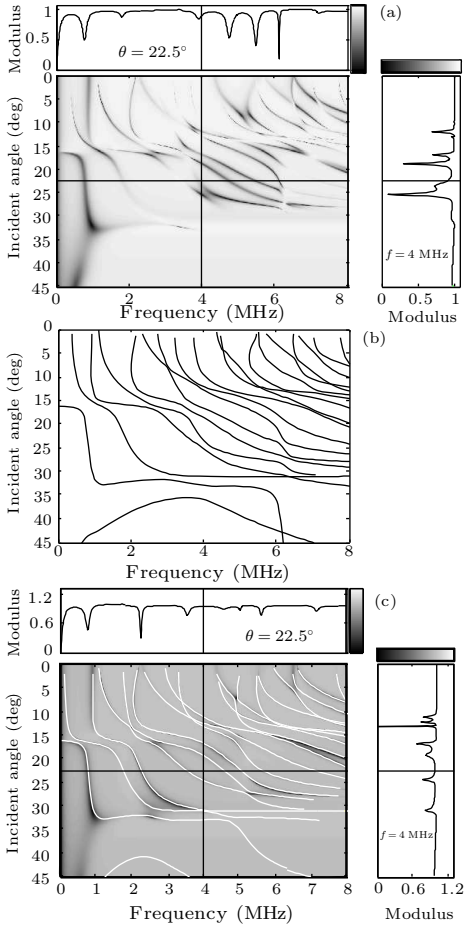

Fig. 1. Comparison of the reflection coefficient function $R(\theta, f)$ and the guided wave dispersion curves for a three-layer aluminum (1.416 mm thickness)-epoxy resin (0.132 mm)-aluminum (0.544 mm). (a) Modulus of $R(\theta, f)$ for the water immersed structure with two perfect interfaces ($k_{\rm t} = \infty$). (b) Mode dispersion curves of the structure without charge (in vacuum). (c) Superposition of $|R(\theta, f)|$ and the dispersion curves of the same structure with the upper interfacial stiffness $k_{\rm t} = 10^{12}\,{\rm N/m^3}$.

Figure 1 gives the reflectance function $R(\theta, f)$ and its comparison with the guided wave dispersion curves for an aluminum-epoxy resin-aluminum adhesively bonded structure used in this study. For these two being directly comparable, the phase velocity $v_{\rm p}$ of the guided waves is transformed into the incident angle θ by the relation $\theta = \sin^{-1}(v_0/v_{\rm p})$, where v_0 is the wave velocity in the charging liquid (water). Figures 1(a) and 1(b) are the modulus of $R(\theta, f)$ and the dispersion curves for the three-layer structure with a perfect adhesion condition ($k_{\rm t} = \infty$) at the two interfaces, while Fig. 1(c) is the superposition of these two for the structure with its upper interface having a weak stiffness ($k_{\rm t} = 10^{12}\,{\rm N/m^3}$).

The $V(z)$ technique has been originally developed in acoustic microscopy to obtain a local measurement of surface wave velocity for imaging the elastic contrast of a sample.[10] It refers to the measurement of the transducer response V at an acoustic lens as a function of the normal distance z between the lens and a testing sample. Working in the tone-burst mode, the interference between the normal reflection and the surface wave leaky results in a periodicity in the amplitude of $V(z)$ output from which the surface wave velocity can be derived.[11] If the sample is a layered structure, no periodicity will exist,[12] and the multimode guided waves can be generated, whose incident angles are covered within the angular aperture of the focus lens (see Fig. 2). In this case, either the time resolved signal $V(z, t)$ or frequency scanning has been employed to obtain $V(z, f)$.[13] An inversion algorithm can be established permitting the reconstruction of the angular and frequency reflection coefficient function $R(\theta, f)$ from $V(z, f)$. The algorithm demonstration can be found in Refs. [14,15]. The direct relation and its inversion are given by

$$V(z, f) = \int_{-\infty}^{\infty} P(\theta, f) R(\theta, f) e^{-j4\pi f z \cos\theta / v_0} d\theta, \tag{1}$$

$$R(\theta, f) = \frac{\int_{-\infty}^{\infty} V(z, f) e^{j4\pi f z \cos\theta / v_0}}{P^*(\theta, f)}, \tag{2}$$

where $P(\theta, f)$ is a function depending only on the properties of the lens, characterizing the angular aperture of the focus beam and the transducer frequency bandwidth in which the reflectance function $R(\theta, f)$ can be reconstructed, $P^*(\theta, f)$ is different from $P(\theta, f)$ according to the lens geometry (point or line focus). For $V(z)$ measurement, $P^*(\theta, f)$ is the lens deconvolution function that has the role to calibrate the lens response or normalize the inverted $R(\theta, f)$. This function can be determined by measuring a $V(z)$ response $V_0(z, f)$ obtained on an acoustic reflector having uniform reflectance $R(\theta, f)$=const=1. From Eq. (2), we have

$$P^*(\theta, f) = \int_{-\infty}^{\infty} V_0(z, f) e^{j4\pi f z \cos\theta / v_0} dz. \tag{3}$$

Compared with other mode waves measurement techniques (such as the laser technique), the $V(z)$ reconstruction method presents several advantages: (i) it is a local measurement avoiding the effect of attenuation of guided waves at high frequency; (ii) it is a multi-wave modes measurement; and (iii) it uses a single transducer and simple experimental setup compared with other traditional measurement methods (such as the pitch-patch technique).

The experimental setup for $V(z)$ inversion is shown in Fig. 3. The instruments employed consist of a pulser/receiver (Olympus 5058PR), a step motor

(driver Newport MM4006 ILS-100MVTP), and a digital oscilloscope (Tektronix TDS3032). The line focus lens used in this work has a central frequency of 5 MHz, a half angular aperture of 45°, a focal length of 25 mm and a transducer width of 10 mm.

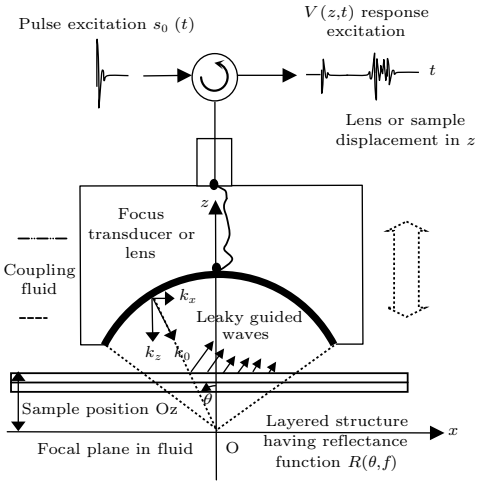

Fig. 2. Principle and schematic diagram of $V(z)$ inversion.

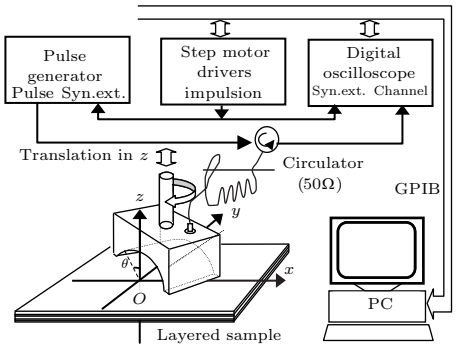

Fig. 3. Experimental setup for the $V(z)$ measurement.

Figure 4 presents an example of registered $V(z,t)$ data and its Fourier transform $V(z,f)$. In practice, the relative translation in z-direction between the lens and the sample has only a finite range. The integrals in Eqs. (1)–(3) are limited in positive z by a defocusing distance $z_{\max}$ between the focal plane and the lens surface, and in negative z by taking 2 or 3 times the length of $z_{\max}$. In Fig. 4(a), the time delay in signals $V(z,t)$ introduced by the translation in z are compensated for by a quantity of $\Delta\tau_i = 2i\Delta z/v_0$, where Δz is the step in z, and i is the step number between the lens and the sample. The inversion of the reflectance function can be numerically calculated by

$$\begin{aligned}|R(\theta_n, f_m)| &= |\sum_{z_i} V(z_i, f_m) e^{j[2\pi f_m (t_0+\Delta\tau_i)]} \\ &\quad \cdot e^{j[4\pi f_m (z_0+z_i)\cos\theta_n / v_0]} \Delta z| \\ &= |\sum_{z_i} V(z_i, f_m) e^{j4\pi f_m z_i (1+\cos\theta_n)/v_0} \Delta z|, \end{aligned} \tag{4}$$

which means that the time reference t_0 and the position reference z_0 during the experimental acquisition will have no effect on the inversion of the reflectance function $R(\theta, f)$ in its modulus.

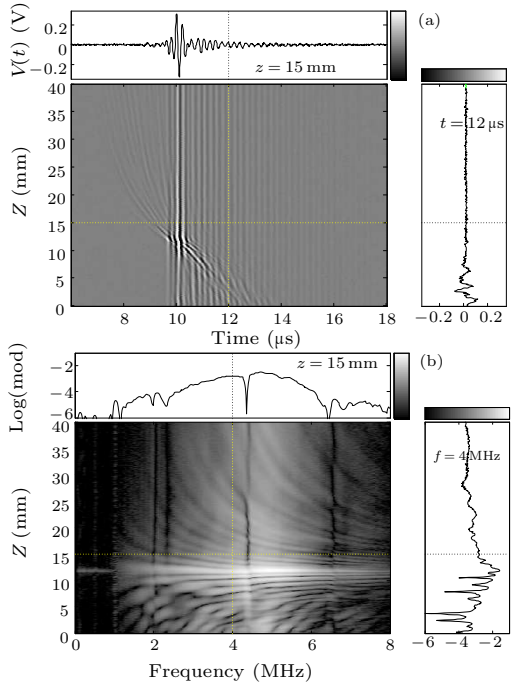

Fig. 4. Experimental $V(z)$ data: (a) $V(z,t)$ signals (time sampling rate=100 MHz; z sampling step $\Delta z = 75$ µm); (b) $V(z,f)$ function obtained by performing Fourier transform of $V(z,t)$ at each z position (frequency resolution $\Delta f = 0.02$ MHz).

Table 1. The sandwich structure adhesive samples with different interfacial bonding qualities.

Samples	Upper Al layer	Upper interface	Middle adhesive layer	Lower interface	Lower Al layer
#1 Good	1.42 mm	good	0.132 mm	good	0.55 mm
#2 Weak	1.42 mm	week	0.147 mm	good	0.557 mm

For interface adhesion evaluation, several adhesive bonding samples have been prepared in the laboratory. They are realized by adhering two aluminum plates (type 1060D) of different thicknesses with an adhesive of epoxy resin (type AD850), which is a typical sandwich structure. The aluminum has such material properties: longitudinal wave velocity $c_{\mathrm{l,Al}} = 6212$ m/s, shear wave velocity $c_{\mathrm{t,Al}} = 3110$ m/s and mass density $\rho_{\mathrm{Al}} = 2699\,\mathrm{kg/m^3}$; those of epoxy-resin are $c_{\mathrm{l,epoxy}} = 2200$ m/s, $c_{\mathrm{t,epoxy}} = 920$ m/s and $\rho_{\mathrm{epoxy}} = 1280\,\mathrm{kg/m^3}$. A good interface adhesion is ensured by a careful cleaning of the aluminum surfaces to be adhered. A weak interface adhesion is simulated by sputtering on the surface a thin layer

(several μm) Teflon (PTFE). The samples have a size of 25 cm × 20 cm and the thickness of each layer constituting the structure is listed in Table 1. There is a slight difference in the thickness of the aluminum plates and the adhesive layers for different samples. They are determined experimentally by measuring the time of flight by using echography with a 50 MHz acoustic lens.

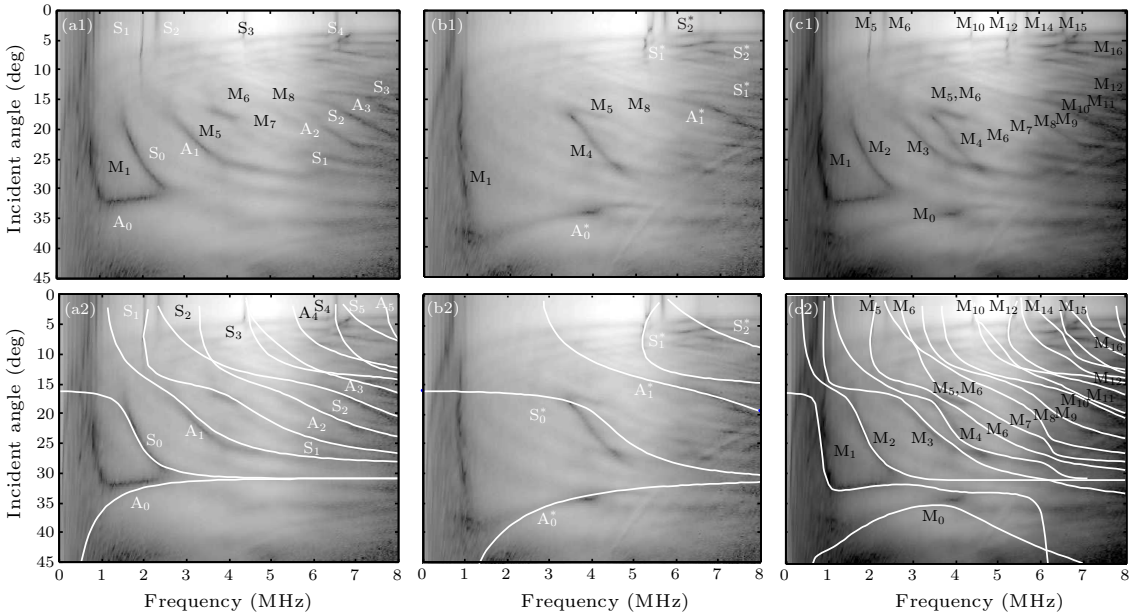

Fig. 5. The inverted reflectance function $|R(\theta, f)|$ and its comparison with the guided wave dispersion curves of the sample #1 having a 'good' adhesion for the two interfaces: (a1) $|R(\theta, f)|$ obtained at the thicker aluminum side; (a2) comparison with the calculated Lamb wave dispersion curves of the single thicker aluminum layer; (b1) $|R(\theta, f)|$ obtained at the thinner aluminum side of the sample; (b2) comparison with the calculated Lamb wave dispersion curves of the single thinner aluminum layer; (c1) fusion of $|R(\theta, f)|$ of (a1) and (a2); and (c2) comparison with the calculated guided wave dispersion curves of the sample with a perfect interface stiffness $k_t = \infty$.

Figure 5 presents the $V(z)$ inversion results obtained on the sample #1. Figures 5(a1) and 5(b1) show the inverted $|R(\theta, f)|$ obtained by $V(z)$ acquisition at the sample side having a thick aluminum layer and at the side having a thin aluminum layer. The two reconstructed $|R(\theta, f)|$'s do not have similar wave modes. Most of the identified mode branches in the $|R(\theta, f)|$ obtained at the thicker aluminum layer side correspond to the Lamb wave modes for the single thick aluminum layer (labeled A_i and S_i); those obtained at the thin aluminum layer side correspond to the Lamb wave modes for the single thin layer (labeled A_i^* and S_i^*). Figures 5(a2) and 5(b2) are the comparison between $|R(\theta, f)|$ and the Lamb wave dispersion curves of their corresponding single layer. By the fusion of these two $|R(\theta, f)|$'s, which is their logarithmic summation, the result given in Fig. 5(c1) represents hence the $V(z)$ inversion for the whole sandwich sample. Figure 5(c2) is the superposition of the fused $|R(\theta, f)|$ and the guided wave dispersion curves calculated for the sample having 'perfect' interface stiffness ($k_t = \infty$) at the both interfaces. In the latter case, the modes cannot be labeled as A_i and S_i like the Lamb wave modes for a single layer but as M_i (for i from 0 to 16) due to the non-symmetricity of the three-layer structure in its thickness. There is a good coincidence between the reconstructed $|R(\theta, f)|$'s and the guided wave dispersion curves, confirming the good interface adhesion of the sample #1.

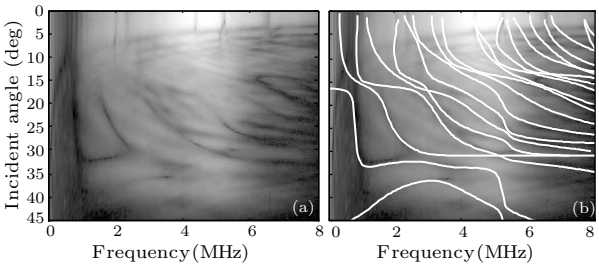

Fig. 6. The inverted reflectance function $|R(\theta, f)|$ and its comparison with the guided wave dispersion curves of the sample #2 having a 'weak' adhesion at the thicker aluminum-adhesive interface: (a) fusion of the $|R(\theta, f)|$ obtained at the two sides of the sample; (b) comparison with the calculated guided wave dispersion curves of the sample having a weak interface stiffness $k_t = 10^{14}$ N/m^3 at the thicker aluminum–adhesive interface.

Figure 6 shows the results for the sample #2. Figures 6(a) and 6(b) are the fused inversion of $|R(\theta, f)|$ and its superposition with the guided wave dispersion curves calculated for the structure having an imperfect interface stiffness k_t at its upper interface. They are obtained after several simulations and comparisons from which the best fitting between $|R(\theta, f)|$ and the mode dispersion corresponds to a k_t value

of $10^{14}\,\mathrm{N/m^3}$. Such a k_t can be considered as a mean weak adhesion of the interface because a completely slipped or a strong adhered interface has a k_t value inferior to $10^{11}\,\mathrm{N/m^3}$ or superior to $10^{18}\,\mathrm{N/m^3}$, respectively.

In conclusion, the angular and frequency reflectance function $|R(\theta, f)|$ can be used for the nondestructive evaluation of the interface adhesion in an adhesively bonded layered structure by analyzing its minima evolution corresponding to the guided wave dispersion of the structure. The shear interfacial stiffness parameter k_t describing the interface adhesion quality has been determined by comparing the measured $R(\theta, f)$ with the calculated guided wave dispersion curves under their best fitting. The $V(z)$ inversion technique is an efficient and practical approach for $R(\theta, f)$ function measurement. The value of $R(\theta, f)$ has to be reconstructed by $V(z)$ inversion on the two sides of the sample. Though the k_t value has been determined to be infinite for an interface with good adhesion and to be $10^{14}\,\mathrm{N/m^3}$ for a weak interface, more measurements must be carried out for a series of samples having different levels of the interface adhesion to confirm this conclusion.

We acknowledge Dr. Xu Yan-Feng in Ultrasonic Lab at Tongji University for his help in the experimental implementation.

References

[1] Brown H R 2000 *Mater. Forum* **24** 49
[2] Awaja F, Gilbert M, Kelly G, Fox B and Pigram P J 2009 *Prog. Poly. Sci.* **34** 948
[3] Veselovsky R A and Kestelman V N 2002 *Adhesion Polymers* (New York: McGraw-Hill) chap 9 p 342
[4] Li M X, Wang X M and An Z W 2013 *Appl. Acoust.* **32** 190 (in Chinese)
[5] Pilarski A and Rose J L 1988 *J. Appl. Phys.* **63** 300
[6] Pialucha T and Cawley P 1994 *J. Acoust. Soc. Am.* **96** 1651
[7] Baik J M and Thompson R B 1984 *J. Nondestr. Eval.* **4** 177
[8] Chimenti D E and Rokhlin S I 1990 *J. Acoust. Soc. Am.* **88** 1603
[9] Crom B L and Castaings M 2010 *J. Acoust. Soc. Am.* **127** 2220
[10] Atalar A 1978 *J. Appl. Phys.* **49** 5130
[11] Kushibiki J I and Chubachi N 1985 *IEEE Trans. Sonics Ultrason.* **SU-32** 189
[12] Xü W J and Ourak M 1997 *NDT&E Int.* **30** 75
[13] Xü W J, Ourak M, Lematre M and Bourse G 2000 *AIP Conference Proceedings* (Montreal, Canada 25–30 July 1999) p 1183
[14] Liang K K, Kino G S and Khuri-Yakub B T 1985 *IEEE Trans. Sonics Ultrason.* **SU-32** 213
[15] Bourse G, Xü W J, Mouftiez A, Vandevoorde L and Ourak M 2012 *NDT&E Int.* **45** 22